

Finite Elements with Divergence-free Shape Function and the Application to Inhomogeneously-loaded Waveguide Analysis

Zaheed MAHMOOD* and Yukio KAGAWA*

(Received October 2, 1995)

Divergence-free shape functions are proposed for the finite elements, with which inhomogeneously-loaded and arbitrarily-shaped waveguides are analysed. The method is based on vectorial finite element formulation employing edge elements. The shape functions used for the approximation of the fields are shown analytically to be divergence-free and as an evidence, the non-physical solutions that appeared in the longitudinal component finite element formulation have been shown to be absent. To show the validity of the elements, application is made for the analysis of rectangular waveguides loaded with dielectric slab and a waveguide with curved structure. The solutions obtained are compared with the analytical ones or the solutions reported elsewhere. The degree of accuracy has been found satisfactory.

1. INTRODUCTION

The finite element method has been widely used for the analysis of waveguide components and is considered to be one of the most powerful and versatile methods for the solution of a wide variety of waveguide problems. In the design of the structures, it is important to calculate the propagation characteristic of the guided modes or the eigenfrequencies of the cross-section. However, the finite element analysis of electromagnetic problems is well known to be plagued by the occurrence of non-physical or spurious solutions. One of the earliest reports on these spurious solutions was by Daly [1], who used axial components for the elements. Several methods have been proposed to suppress these spurious solutions. One of the earliest proposal to identify these spurious modes, made by Davies [2] was to include the square of the divergence of the field in the variational formulation. The subsequent headway was made by Rahman [3], Webb [4] and Koshiba [5] and others, who introduced a penalty term in the formulation which enforces the constraint $\nabla \cdot \mathbf{E} = 0$ in the formulation. This constraint has empirically been found to suppress the spurious modes and in some cases, this only pushes the spurious modes out of the region of interest. This technique involves an arbitrary positive constant, called the penalty coefficient and the accuracy of the solution depends on its magnitude. As to the formulation, Hayata [6] used three components of the magnetic field where the axial component (z direction) is expressed in terms of the transverse components, satisfying the condition of zero divergence. Lee [7] obtained the formulation providing the multiplicity of the set of zero eigenvalues set to a finite number known in advance, yielding approximation of the zero eigenvalues with good accuracy.

Kobelansky and Webb [8] proposed the use of the basis functions in the elements with which the fields are exactly divergence-free. These divergence-free basis functions are obtained by solving an auxiliary eigen-matrix system in which intensive computations are required since at least tens of basis functions are needed to be calculated. The present method

* Department of Electrical and Electronic Engineering

proposes the use of the shape functions which does not need any pre-fixing but is inherently divergence-free. This means that the present shape functions accommodate straightforwardly the zero divergence of the field in the formulation in an explicit way and get rid of the spurious solutions resulting from the non-compliance with divergence-free condition. The analytical proof of its divergence-free condition is given in section 4.

2. BASIC EQUATION AND VARIATIONAL FORMULATION

Considering a metallic-walled waveguide with closed cross-section Ω , the source-free Maxwell's equations with time dependence of $\exp(j\omega t)$ being implied are given by

$$\nabla \times \mathbf{E} = -j\omega\mu_0\mu_r\mathbf{H} \quad (1)$$

$$\nabla \times \mathbf{H} = j\omega\epsilon_0\epsilon_r\mathbf{E} \quad (2)$$

where ω is the angular frequency, ϵ_0 and μ_0 are the permittivity and permeability of free space, respectively, and ϵ_r and μ_r are the corresponding relative material properties. At the interface between two contiguous media i and j , the following conditions must be satisfied:

$$\mathbf{n} \times \mathbf{E}_i = \mathbf{n} \times \mathbf{E}_j \quad (3a)$$

$$\mathbf{n} \times \mathbf{H}_i = \mathbf{n} \times \mathbf{H}_j \quad (3b)$$

$$\mathbf{n} \cdot \mathbf{D}_i = \mathbf{n} \cdot \mathbf{D}_j \quad (3c)$$

$$\mathbf{n} \cdot \mathbf{B}_i = \mathbf{n} \cdot \mathbf{B}_j \quad (3d)$$

where \mathbf{B} and \mathbf{D} are respectively the magnetic and electric flux density and \mathbf{n} is the interface normal unit vector. On the boundary of the domain Ω , the appropriate boundary conditions are:

$$\mathbf{n} \times \mathbf{E} = 0 \quad (3e)$$

$$\mathbf{n} \cdot \mathbf{B} = 0 \quad (3f)$$

on the perfect electric walls and

$$\mathbf{n} \times \mathbf{H} = 0 \quad (3g)$$

$$\mathbf{n} \cdot \mathbf{D} = 0 \quad (3h)$$

on the perfect magnetic walls.

The above Eqs. (1)-(3) describe the classical boundary-value problem unambiguously, where part of the equations are dealt with in a straightforward manner while the rest of those are satisfied naturally. The Maxwell's equations given by Eqs. (1) and (2) and the equations of tangential boundary conditions given by Eqs. (3a), (3b), (3e) and (3g) are used directly in solving the problem within the prescribed domain while at the same time solutions to them implicitly satisfy the Maxwell's divergence equation $\nabla \cdot \mathbf{B} = 0$ and $\nabla \cdot \mathbf{D} = 0$ and the normal boundary conditions given by Eqs. (3c), (3d), (3f) and (3h).

By taking the curl of both sides of the Eq. (1) and then substituting Eq. (2) into (1), the following vectorial wave equation for \mathbf{E} is derived:

$$\mu_r^{-1} \nabla \times (\nabla \times \mathbf{E}) - k_0^2 \epsilon_r \mathbf{E} = 0 \quad \text{in } \Omega \quad (4)$$

$$\text{where} \quad k_0^2 = \omega^2 \epsilon_0 \mu_0 \quad (5)$$

The following functional (6) can easily be obtained from Eq. (4) when there is no energy flow across the boundary and it has been proved [9] that the functional given by Eq. (6) is stationary about the correct solutions:

$$L(\mathbf{E}) = \int_{\Omega} \{ (\mu_r^{-1} \nabla \times \mathbf{E})^* \cdot (\nabla \times \mathbf{E}) - k_0^2 \epsilon_r \mathbf{E}^* \cdot \mathbf{E} \} d\Omega \quad (6)$$

where the asterisk denotes the complex conjugate.

3. FINITE ELEMENT FORMULATION

The cross-section of a waveguide is divided into the finite elements of simple geometric shape to approximate the domain. Thus, we seek an approximate solution for the domain with a suitable finite element mesh. The finite element meshes consist of triangular or quadrilateral elements, that allow unique derivation of the interpolation functions. For edge elements, the elements are connected to each-other by sharing the common edges on the boundaries of the elements. Hano [10] has used rectangular edge elements and Kikuchi [11] and Koshiba [12] have used triangular edge elements. Koshiba has shown the tangential components to be continuous along the inter-element boundaries and constant on each side of triangles. Hano and Koshiba's formulations have been developed for solving inhomogeneous waveguiding problems whereas Kikuchi's one is for homogeneous hollow waveguiding problems. We here use triangular edge elements [13] where the shape functions are chosen to be analytically non-divergent, which are different from the ones used by the above authors. However, even though Koshiba's element [12] is also analytically divergence-free, the present shape function can be presented by expression which are simpler compared (see appendix) to Koshiba's.

3.1 Triangular edge elements

The domain of the problem is here divided into triangular elements, in each of which the material property is constant. Within the element, the electric field \mathbf{E} is approximated by the linear combination as

$$\mathbf{E}(x,y,z) = [\mathbf{F}]^T \{ \phi \}_e \quad (7)$$

$$\text{or, } E_x = \{F_x\} \{ \phi_t \}_e, \quad E_y = \{F_y\} \{ \phi_t \}_e \quad \text{and } E_z = j\{N\} \{ \phi_z \}_e \quad (7)'$$

$$\text{where } \{ \phi \}_e = \begin{bmatrix} \{ \phi_t \}_e \\ \{ \phi_z \}_e \end{bmatrix} \quad \text{with } \{ \phi_t \}_e = \begin{bmatrix} \phi_{t1} \\ \phi_{t2} \\ \phi_{t3} \end{bmatrix} \quad \text{and } \{ \phi_z \}_e = \begin{bmatrix} \phi_{z1} \\ \phi_{z2} \\ \phi_{z3} \end{bmatrix} \quad (8)$$

and

$$[\mathbf{F}] = \begin{bmatrix} \{F_x\} & \{F_y\} & \{0\} \\ \{0\} & \{0\} & j\{N\} \end{bmatrix} \quad \text{where } \{F_x\} = \begin{bmatrix} N_{12}^x + N_{21}^x \\ N_{23}^x + N_{32}^x \\ N_{31}^x + N_{13}^x \end{bmatrix}^T \quad \text{and } \{F_y\} = \begin{bmatrix} N_{12}^y + N_{21}^y \\ N_{23}^y + N_{32}^y \\ N_{31}^y + N_{13}^y \end{bmatrix}^T \quad (9)$$

In Eq.(8), the set of unknowns of tangential components ϕ_{t1} , ϕ_{t2} and ϕ_{t3} and axial components ϕ_{z1} , ϕ_{z2} and ϕ_{z3} are defined on the edges and the nodes respectively of the triangle as shown in Fig.1(a). Besides, N_{ij}^x and N_{ij}^y , the components of $\{F_x\}$ and $\{F_y\}$ respectively, are x and y directed components of the vector shape function N_{ij} , such that $N_{ij} = iN_{ij}^x + jN_{ij}^y$, where i and j are the unit vectors along x and y directions respectively of the rectangular coordinate system. The vector shape functions N_{ij} are given by

$$N_{23} = \frac{\mathbf{n}_3}{\mathbf{a}_1 \cdot \mathbf{n}_3} N_2 \quad N_{31} = \frac{\mathbf{n}_1}{\mathbf{a}_2 \cdot \mathbf{n}_1} N_3 \quad N_{12} = \frac{\mathbf{n}_2}{\mathbf{a}_3 \cdot \mathbf{n}_2} N_1$$

$$N_{32} = \frac{\mathbf{n}_2}{\mathbf{a}_1 \cdot \mathbf{n}_2} N_3 \quad N_{13} = \frac{\mathbf{n}_3}{\mathbf{a}_2 \cdot \mathbf{n}_3} N_1 \quad N_{21} = \frac{\mathbf{n}_1}{\mathbf{a}_3 \cdot \mathbf{n}_1} N_2 \quad (10)$$

where 'a's are the unit vectors defined along the edges and 'n's are the unit normals defined on the corresponding edges of the triangle as shown in Fig. 1(b), and 'N's are the area coordinates ($\sum N_i=1$, $i=1$ to 3). The shape function component N_{ij} , defined along the edge with unit vector \mathbf{a}_k , is the contribution from the side of node i , and the tangential shape function $F(F_x, F_y)$, defined along an edge is made of the components (defined by Eq. (10)) contributed from the two nodes joining that edge.

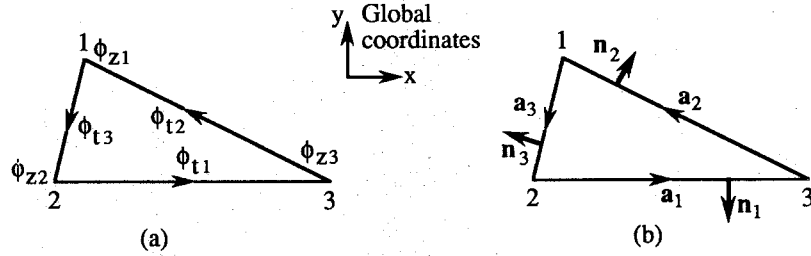


Fig. 1 Present triangular edge element showing location of (a) tangential and axial unknowns and (b) unit vectors along the edges and normal to the edges.

Here, the electric field is assumed to have a z dependence as $E(x,y) \exp(-j\beta z)$, where β is the propagation constant.

Substituting Eqs.(7)-(10) in Eq.(6), and making the functional stationary for element e , we obtain

$$[\mathbf{K}]_e \{\phi\}_e - k_0^2 [\mathbf{M}]_e \{\phi\}_e = \{0\} \quad (11)$$

where

$$[\mathbf{K}]_e = \int_{\Omega_e} \begin{bmatrix} \left(\frac{\partial F_y}{\partial x} - \frac{\partial F_x}{\partial y} \right) \left(\frac{\partial F_y}{\partial x} - \frac{\partial F_x}{\partial y} \right)^T & \beta \left(\{F_x\} \frac{\partial N}{\partial x} + \{F_y\} \frac{\partial N}{\partial y} \right)^T \\ \beta^2 \left(\{F_x\} \{F_x\}^T + \{F_y\} \{F_y\}^T \right) & \\ \beta \left(\{F_x\} \frac{\partial N}{\partial x} + \{F_y\} \frac{\partial N}{\partial y} \right) & \frac{\partial N}{\partial x} \frac{\partial N}{\partial x} + \frac{\partial N}{\partial y} \frac{\partial N}{\partial y} \end{bmatrix} dx dy$$

$$[\mathbf{M}]_e = \int_{\Omega_e} \begin{bmatrix} \{F_x\} \{F_x\}^T + \{F_y\} \{F_y\}^T & (0) \\ (0) & \{N\} \{N\}^T \end{bmatrix} dx dy$$

Eq.(11) can be resolved into

$$\int_{\Omega_e} \left[\beta^2 \left(\{F_x\} \{F_x\}^T + \{F_y\} \{F_y\}^T \right) \{\phi_t\}_e + \left(\frac{\partial F_y}{\partial x} - \frac{\partial F_x}{\partial y} \right) \left(\frac{\partial F_y}{\partial x} - \frac{\partial F_x}{\partial y} \right)^T \{\phi_t\}_e \right. \\ \left. + \beta \left(\{F_x\} \frac{\partial N}{\partial x} + \{F_y\} \frac{\partial N}{\partial y} \right) \{\phi_z\}_e - k_0^2 \left(\{F_x\} \{F_x\}^T + \{F_y\} \{F_y\}^T \right) \{\phi_t\}_e \right] dx dy = 0$$

$$\text{and} \int_{\Omega_e} \left[\beta \left(\{F_x\} \frac{\partial \{N\}^T}{\partial x} + \{F_y\} \frac{\partial \{N\}^T}{\partial y} \right) \{ \phi_t \}_e + \left(\frac{\partial \{N\}}{\partial x} \frac{\partial \{N\}^T}{\partial x} + \frac{\partial \{N\}}{\partial y} \frac{\partial \{N\}^T}{\partial y} \right) \{ \phi_z \}_e - k_0^2 \left(\{N\} \{N\}^T \right) \{ \phi_z \}_e \right] dx dy = 0 \quad (12)$$

Rearranging the terms of Eq.(12), we obtain,

$$\begin{aligned} & \int_{\Omega_e} \left[k_0^2 \left(\{F_x\} \{F_x\}^T + \{F_y\} \{F_y\}^T \right) \{ \phi_t \}_e - \left(\frac{\partial \{F_y\}}{\partial x} - \frac{\partial \{F_x\}}{\partial y} \right) \left(\frac{\partial \{F_y\}}{\partial x} - \frac{\partial \{F_x\}}{\partial y} \right)^T \{ \phi_t \}_e \right. \\ & \left. - \beta \left(\{F_x\} \frac{\partial \{N\}^T}{\partial x} + \{F_y\} \frac{\partial \{N\}^T}{\partial y} \right) \{ \phi_z \}_e - \beta^2 \left(\{F_x\} \{F_x\}^T + \{F_y\} \{F_y\}^T \right) \{ \phi_t \}_e \right] dx dy = 0 \\ & \int_{\Omega_e} \left[-\beta \left(\{F_x\} \frac{\partial \{N\}^T}{\partial x} + \{F_y\} \frac{\partial \{N\}^T}{\partial y} \right) \{ \phi_t \}_e + \left(k_0^2 \{N\} \{N\}^T - \frac{\partial \{N\}}{\partial x} \frac{\partial \{N\}^T}{\partial x} - \frac{\partial \{N\}}{\partial y} \frac{\partial \{N\}^T}{\partial y} \right) \{ \phi_z \}_e \right] dx dy = 0 \end{aligned} \quad (13)$$

Eq.(13) can be considered for all the elements and expressed by a system of matrix equation as follows

$$\begin{aligned} [S_{tt}] \{ \phi_t \} - \beta [S_{tz}] \{ \phi_z \} - \beta^2 [M_{tt}] \{ \phi_t \} &= 0 \\ -\beta [S_{zt}] \{ \phi_t \} + [S_{zz}] \{ \phi_z \} &= 0 \end{aligned} \quad (14)$$

where $\{ \phi_t \}$ and $\{ \phi_z \}$ are the global unknowns,

$$\begin{aligned} [S_{tt}] &= \sum_e \int_{\Omega_e} \left[k_0^2 \left(\{F_x\} \{F_x\}^T + \{F_y\} \{F_y\}^T \right) - \left(\frac{\partial \{F_y\}}{\partial x} - \frac{\partial \{F_x\}}{\partial y} \right) \left(\frac{\partial \{F_y\}}{\partial x} - \frac{\partial \{F_x\}}{\partial y} \right)^T \right] dx dy \\ [S_{tz}] &= \sum_e \int_{\Omega_e} \left[\left(\{F_x\} \frac{\partial \{N\}^T}{\partial x} + \{F_y\} \frac{\partial \{N\}^T}{\partial y} \right) \right] dx dy = [S_{zt}]^T \\ [S_{zz}] &= \sum_e \int_{\Omega_e} \left[\left(k_0^2 \{N\} \{N\}^T - \frac{\partial \{N\}}{\partial x} \frac{\partial \{N\}^T}{\partial x} - \frac{\partial \{N\}}{\partial y} \frac{\partial \{N\}^T}{\partial y} \right) \right] dx dy \\ [M_{tt}] &= \sum_e \int_{\Omega_e} \left[\left(\{F_x\} \{F_x\}^T + \{F_y\} \{F_y\}^T \right) \right] dx dy \end{aligned} \quad (15)$$

Following the way described in Ref.(12), from the two matrix equations of Eq.(14), the following eigenvalue equation can be obtained where the unknowns to be resolved are consist of tangential components only.

$$\left([S_{tt}] - \beta^2 [K_{tt}] \right) \{ \phi_t \} = 0 \quad \text{where} \quad [K_{tt}] = [S_{tz}] [S_{zz}]^{-1} [S_{zt}] + [M_{tt}] \quad (16)$$

Eq.(16) can easily be solved by standard eigenvalue solver which yield directly the propagation constant as the eigenvalues.

4. DIVERGENCE-FREE SHAPE FUNCTION AND ITS ANALYTICAL PROOF

By now, it has been well established that a non-compliance with the divergence-free condition has always appeared to be an origin of non-physical solutions. This phenomenon is quite evident while the spurious modes encountered by the conventional elements have been found to be suppressed by incorporation of zero-divergence of the field in the original formulation by Penalty [3] or Lagrange multiplier [13] method. The present element is found to encounter spurious-free solutions. The reason behind that is, the element has been found to be non-divergent. This means that the condition of zero-divergence of the field incorporated externally in order to suppress the spurious modes by Penalty or Lagrange multiplier method has been applied naturally in an inherent manner in the present element employed. The analytical proof of non-divergence in the present element is furnished as follows:

The divergence of the present shape function (Eq.(9)) is given by

$$\nabla \cdot [F]^T = \nabla \cdot \begin{bmatrix} \{F_x\} & \{F_y\} & \{0\} \\ \{0\} & \{0\} & j\{N\} \end{bmatrix}^T = \begin{bmatrix} \frac{\partial \{F_x\}}{\partial x} + \frac{\partial \{F_y\}}{\partial y} \\ \frac{j\partial \{N\}}{\partial z} \end{bmatrix}^T$$

As N doesn't have any derivatives along z direction, we are left with tangential shape function $F(F_x, F_y)$, so that for the edge 2-3 of the triangle shown in Fig.1(b), we can write the divergence of the shape function using Eqs.(9)-(10) as

$$\nabla \cdot F_{23} = \nabla \cdot (N_{23} + N_{32}) = \frac{\mathbf{n}_3 \cdot \mathbf{i}}{\mathbf{a}_1 \cdot \mathbf{n}_3} \frac{\partial N_2}{\partial x} + \frac{\mathbf{n}_3 \cdot \mathbf{j}}{\mathbf{a}_1 \cdot \mathbf{n}_3} \frac{\partial N_2}{\partial y} + \frac{\mathbf{n}_2 \cdot \mathbf{i}}{\mathbf{a}_1 \cdot \mathbf{n}_2} \frac{\partial N_3}{\partial x} + \frac{\mathbf{n}_2 \cdot \mathbf{j}}{\mathbf{a}_1 \cdot \mathbf{n}_2} \frac{\partial N_3}{\partial y} \quad (\text{A1})$$

Here, \mathbf{a} 's are the unit vectors along the edges and \mathbf{n} 's are the unit normals directed outward at the corresponding edges as described in section 3.1 and shown in Fig.1(b) and N 's are the area coordinates. So that F_{23} is defined along the edge with unit vector \mathbf{a}_1 . Each resolved component of (A1) is derived as follows :

$$\begin{aligned} \mathbf{a}_1 \cdot \mathbf{i} &= \frac{x_3 - x_2}{[(x_3 - x_2)^2 + (y_3 - y_2)^2]^{1/2}} ; \mathbf{n}_3 \cdot \mathbf{i} = \frac{y_2 - y_1}{[(x_2 - x_1)^2 + (y_2 - y_1)^2]^{1/2}} ; \mathbf{n}_2 \cdot \mathbf{i} = \frac{y_1 - y_3}{[(x_3 - x_1)^2 + (y_3 - y_1)^2]^{1/2}} \\ \mathbf{a}_1 \cdot \mathbf{j} &= \frac{y_3 - y_2}{[(x_3 - x_2)^2 + (y_3 - y_2)^2]^{1/2}} ; \mathbf{n}_3 \cdot \mathbf{j} = \frac{x_1 - x_2}{[(x_2 - x_1)^2 + (y_2 - y_1)^2]^{1/2}} ; \mathbf{n}_2 \cdot \mathbf{j} = \frac{x_3 - x_1}{[(x_3 - x_1)^2 + (y_3 - y_1)^2]^{1/2}} \end{aligned} \quad (\text{A2})$$

In Eq.(A2), x_i and y_i represent the x and y coordinate respectively at node 'i' of the triangle. Obtaining the derivatives of area coordinate N with respect to x and y for the triangle consisting of nodes 1, 2 and 3, and making some algebraic simplification and considering $d = 2 \times \text{area of triangle}$, we obtain

$$\frac{\mathbf{n}_3 \cdot \mathbf{i}}{\mathbf{a}_1 \cdot \mathbf{n}_3} \frac{\partial N_2}{\partial x} = \frac{(y_2 - y_1)(y_3 - y_1)[(x_3 - x_2)^2 + (y_3 - y_2)^2]^{1/2}}{d[(x_3 - x_2)(y_2 - y_1) + (y_3 - y_2)(x_1 - x_2)]} = \frac{(y_2 - y_1)(y_3 - y_1)[(x_3 - x_2)^2 + (y_3 - y_2)^2]^{1/2}}{d[x_3y_2 - x_3y_1 + x_2y_1 + x_1y_3 - x_2y_3 - x_1y_2]} \quad (\text{A3})$$

$$\text{and } \frac{\mathbf{n}_2 \cdot \mathbf{i}}{\mathbf{a}_1 \cdot \mathbf{n}_2} \frac{\partial N_3}{\partial x} = \frac{(y_1 - y_3)(y_1 - y_2) [(x_3 - x_2)^2 + (y_3 - y_2)^2]^{1/2}}{d[(x_3 - x_2)(y_1 - y_3) + (y_3 - y_2)(x_3 - x_1)]} = \frac{(y_1 - y_3)(y_1 - y_2) [(x_3 - x_2)^2 + (y_3 - y_2)^2]^{1/2}}{-d[x_3y_2 - x_3y_1 + x_2y_1 + x_1y_3 - x_2y_3 - x_1y_2]} \quad (\text{A4})$$

From Eqs.(A3) and (A4) we can write

$$\frac{\mathbf{n}_3 \cdot \mathbf{i}}{\mathbf{a}_1 \cdot \mathbf{n}_3} \frac{\partial N_2}{\partial x} = - \frac{\mathbf{n}_2 \cdot \mathbf{i}}{\mathbf{a}_1 \cdot \mathbf{n}_2} \frac{\partial N_3}{\partial x}$$

or

$$\frac{\mathbf{n}_3 \cdot \mathbf{i}}{\mathbf{a}_1 \cdot \mathbf{n}_3} \frac{\partial N_2}{\partial x} + \frac{\mathbf{n}_2 \cdot \mathbf{i}}{\mathbf{a}_1 \cdot \mathbf{n}_2} \frac{\partial N_3}{\partial x} = 0 \quad (\text{A5})$$

Again, using Eq.(A2) and some algebraic simplification, we obtain

$$\frac{\mathbf{n}_3 \cdot \mathbf{j}}{\mathbf{a}_1 \cdot \mathbf{n}_3} \frac{\partial N_2}{\partial y} = \frac{(x_1 - x_2)(x_1 - x_3) [(x_3 - x_2)^2 + (y_3 - y_2)^2]^{1/2}}{d[x_3y_2 - x_3y_1 + x_2y_1 + x_1y_3 - x_2y_3 - x_1y_2]} \quad (\text{A6})$$

$$\text{and } \frac{\mathbf{n}_2 \cdot \mathbf{j}}{\mathbf{a}_1 \cdot \mathbf{n}_2} \frac{\partial N_3}{\partial y} = \frac{(x_3 - x_1)(x_2 - x_1) [(x_3 - x_2)^2 + (y_3 - y_2)^2]^{1/2}}{-d[x_3y_2 - x_3y_1 + x_2y_1 + x_1y_3 - x_2y_3 - x_1y_2]} \quad (\text{A7})$$

And from Eqs.(A6) and (A7), we can write

$$\frac{\mathbf{n}_3 \cdot \mathbf{j}}{\mathbf{a}_1 \cdot \mathbf{n}_3} \frac{\partial N_2}{\partial y} + \frac{\mathbf{n}_2 \cdot \mathbf{j}}{\mathbf{a}_1 \cdot \mathbf{n}_2} \frac{\partial N_3}{\partial y} = 0 \quad (\text{A8})$$

Adding Eqs.(A5) and (A8) we have

$$\frac{\mathbf{n}_3 \cdot \mathbf{i}}{\mathbf{a}_1 \cdot \mathbf{n}_3} \frac{\partial N_2}{\partial x} + \frac{\mathbf{n}_2 \cdot \mathbf{i}}{\mathbf{a}_1 \cdot \mathbf{n}_2} \frac{\partial N_3}{\partial x} + \frac{\mathbf{n}_3 \cdot \mathbf{j}}{\mathbf{a}_1 \cdot \mathbf{n}_3} \frac{\partial N_2}{\partial y} + \frac{\mathbf{n}_2 \cdot \mathbf{j}}{\mathbf{a}_1 \cdot \mathbf{n}_2} \frac{\partial N_3}{\partial y} = 0 \quad (\text{A9})$$

Comparing Eqs.(A1) and (A9) we get

$$\nabla \cdot \mathbf{F}_{23} = \nabla \cdot (\mathbf{N}_{23} + \mathbf{N}_{32}) = 0 \quad (\text{A10})$$

Applying the same reasoning, the other shape functions of the present element (section 3.1) can be proved divergence-free.

5. NUMERICAL EXAMPLES

To justify that the analytically proven non-divergent elements presented in the previous sections encounter spurious-free solutions, the numerical analysis are carried out by employing the present elements for some sample problems. The solutions are compared with other finite element solutions to examine the quality and accuracy offered by the present elements.

The first example, the structure of which is shown in Fig. 2, is a waveguide where the outer surface is a perfect conductor and a strip of zero thickness is placed in the center. For symmetry, half of the structure is only considered. The dominant mode is a quasi-TEM. Comparison is made for the dominant mode with the longitudinal component formulation by Daly [1]. The dispersion curves are furnished in Fig.3. In Daly's solutions, spurious modes have been reported to

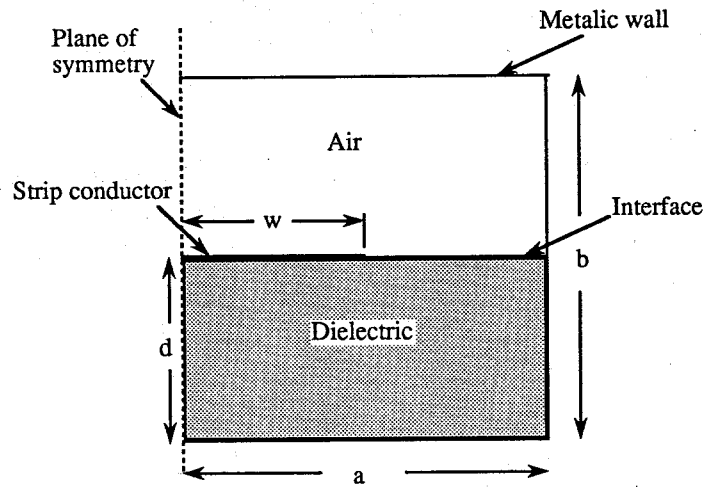


Fig. 2 Cross-sectional structure of the closed micro-strip waveguide with $a = b = 2w = 2d$.

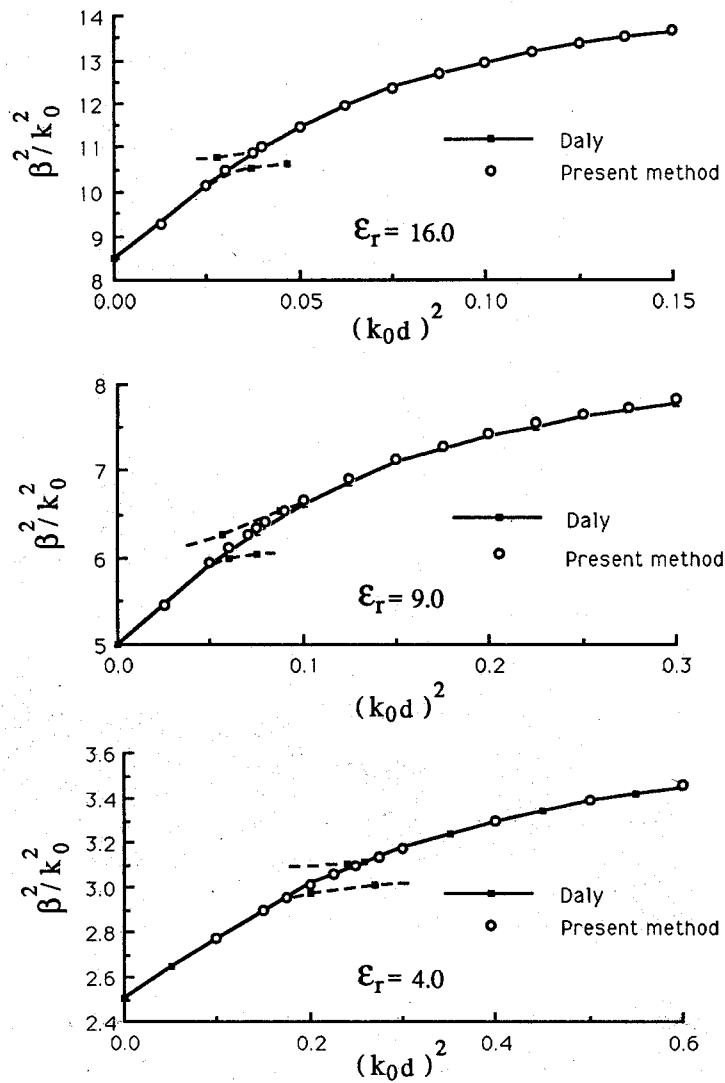


Fig. 3 Comparison of dispersion curves for different permittivity, obtained by Daly's and present method. The dotted lines indicate the deviation in Daly's method.

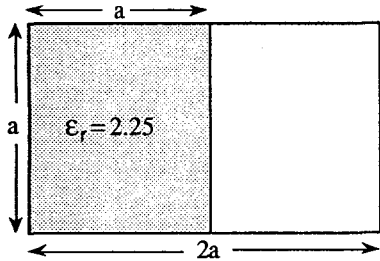


Fig. 4 Structure of a rectangular waveguide with the half loaded with a dielectric slab.

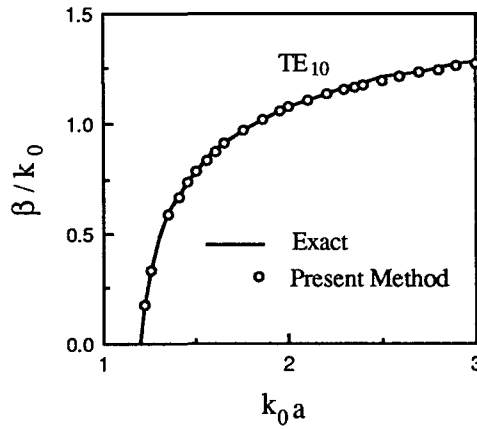


Fig. 5 Dispersion curve for the dominant TE₁₀ mode for the structure of half-loaded dielectric waveguide.

appear along with the physical ones. The dotted lines for Daly's solutions indicate the deviation due to singularity [1]. The solutions obtained by the present method have been found to be completely free of the spurious solutions.

Next, a rectangular waveguide, half of which (Fig.4) is loaded with a dielectric slab is considered. In Fig. 5, the exact dispersion characteristics [14] are compared with the ones obtained by employing the present element for the fundamental TE₁₀ mode. The element divisions taken for the simulation is 8×4. The comparison indicates a good degree of accuracy. The next higher mode is longitudinal section magnetic (LSM) mode for which the dispersion curve obtained by employing the present element is compared in Fig.6 with the one obtained by Angkaew [15]. The present element offers better accuracy than the Angkaew's for the same number of element divisions (8×4).

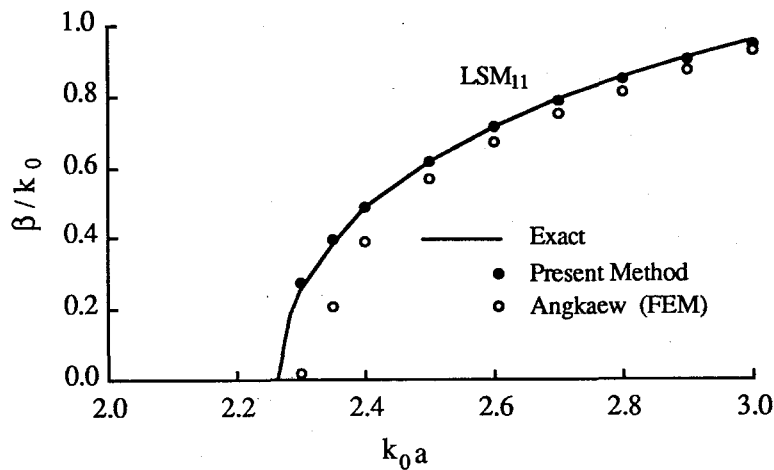


Fig. 6 Comparison of the dispersion curves obtained by this and Angkaew's method for LSM₁₁ mode for the structure of half-loaded dielectric waveguide.

As a test for the applicability of the element to a waveguide with curved boundaries, a hollow circular waveguide of radius 'a' is analyzed. The computation is carried out with the mesh shown in Fig.7 where a quarter of the waveguide is considered with 32 triangular elements. The dispersion characteristics for TM₀₁ and TE₂₁ modes are compared in Fig.8.

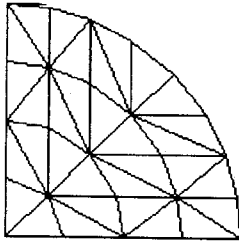


Fig. 7 Finite element mesh of one quarter of a hollow circular waveguide.

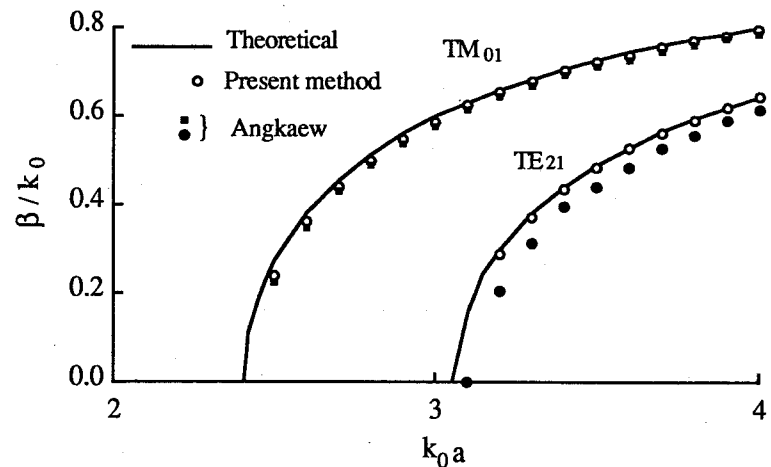


Fig. 8 Dispersion curve for a hollow circular waveguide of radius 'a'.

Angkaew [15] employed 36 first order linear triangular elements. The present elements have been found to yield spurious-free solutions and exhibit better accuracy compared with the one by Angkaew, even for fewer number of elements. Moreover, experience of very low percentage of error for the solutions that correspond to modes upto several higher ones, also validates the use of the present element (shape function) in the analysis of particular waveguiding problem that deals with higher modes.

6. CONCLUSION

A simple finite element that provides divergence-free shape functions is proposed, and its capability is examined for inhomogeneously-loaded arbitrarily shaped waveguiding problem. Employing the present shape functions, the eigenvalue formulation that solves for the propagation constant directly is derived. The shape function used for approximating the field is analytically proven to be non-divergent, and it can completely eliminate the spurious modes originating from the non-compliance with the divergence-free condition implied by Maxwell's equation. As a test, the example of a closed microstrip waveguide known to encounter non-physical solutions when analyzed by the axial component finite element formulation has been tried employing the present formulation. As expected, no spurious modes have been observed. Another merit is that the present shape functions provide good accuracy and convergence characteristics.

REFERENCES

- [1] P. Daly, "Hybrid-mode analysis of microstrip by finite-element methods," *IEEE Trans. Microwave Theory Tech.* vol. 19, (1971), pp.19-25.
- [2] J. B. Davies, F. A. Fernandez and G. Y. Philippou, "Finite element analysis of all modes in cavities with circular symmetry," *IEEE Trans. Microwave Theory Tech.* vol.30, (1982), pp.1975-1979.

- [3] B. M. A. Rahman and J. B. Davies, "Penalty function improvement of waveguide solution by finite elements," *IEEE Trans. Microwave Theory Tech.* vol.32, (1984), pp.922-928.
- [4] J. P. Webb, "The finite-element method for finding modes of dielectric-loaded cavities," *IEEE Trans. Microwave Theory Tech.* vol.33, (1985), pp.635-639.
- [5] M. Koshiba, K. Hayata and M. Suzuki, "Improved finite-element formulation in terms of magnetic field vector for dielectric waveguides," *IEEE Trans. Microwave Theory Tech.* vol. 33, (1985), pp.227-233.
- [6] K. Hayata, M. Koshiba, M. Eguchi and M. Suzuki, "Vectorial finite-element method without any spurious solutions for dielectric waveguiding problems using transverse magnetic-field component," *IEEE Trans. Microwave Theory Tech.* vol. 34, (1986), pp.1120-1124.
- [7] J. F. Lee, D. K. Sun and Z. J. Cendes, "Tangential vector finite elements for electromagnetic field computations," presented at *Fourth Biennial IEEE Conference, Electromagnetic Field Computation*, Toronto, Canada, (1990).
- [8] A. J. Kobelansky and J. P. Webb, "Eliminating spurious modes in finite-element waveguide problems by using divergence-free fields," *Electron Lett.*, vol.22, (1986), pp.569-570.
- [9] A. Konrad, "Vectorial variational formulation of electromagnetic fields in anisotropic media," *IEEE Trans. Microwave Theory Tech.* vol. 24, (1976), pp.553-559.
- [10] M. Hano, "Finite-element analysis of dielectric loaded waveguides," *IEEE Trans. Microwave Theory Tech.* vol. 32, (1984), pp.1275-1279.
- [11] F. Kikuchi, "Mixed and penalty formulations for finite element analysis of an eigenvalue problem in electromagnetism," *Comput. Methods Appl. Mech. Eng.*, vol.64, (1987), pp.509-521.
- [12] M. Koshiba and K. Inoue, "Simple and efficient finite-element analysis of microwave and optical waveguides," *IEEE Trans. Microwave Theory Tech.* vol.40, (1992), pp.371-377.
- [13] T. Yamabuchi, S. Fuji, T. Murai S. Hirose, T. Futagami and Y. Kagawa, "Finite element analysis of electromagnetic fields by using three-dimensional hexagonal edge elements," *IEICE Trans. Institute of Electronics Information and Communication Engineers, Japan*, vol. J75-C-I No.2, (1992), pp.65-73.
- [14] R. E. Collin, *Field theory of guided waves*, McGraw-Hill, New York, (1960).
- [15] T. Angkaew, M. Matsuhara and N. Kumagai, "Finite-element analysis of waveguide modes : A novel approach that eliminates spurious modes," *IEEE Trans. Microwave Theory Tech.* vol. 35, (1987), pp.117-123.

APPENDIX

The vector shape functions employed to approximate the transverse field components can be presented by simple expression. For example, if $\{F_x\}$ of Eq.(7) is expressed as $\{F_x\} = [F_{x1}, F_{x2}, F_{x3}]$, then F_{x1} is given by

$$F_{x1} = (y_1 - y) \times A_1 / d \quad (B1)$$

where A_1 is the length of the triangle-side along which F_{x1} is defined; y_1 is the y coordinate of the vertex of the triangle corresponding to the base A_1 and d equals twice the area of the triangle. The derivation of the expression given by Eq.(B1) is obtained as follows:

As explained in section 3.1, F_{x1} is made of the components of vector shape function given by Eq.(10). Accordingly, for the triangular edge element of Fig.1(b), F_{x1} can be written as

$$F_{x1} = \frac{\mathbf{n}_3 \cdot \mathbf{i}}{\mathbf{a}_1 \cdot \mathbf{n}_3} N_2 + \frac{\mathbf{n}_2 \cdot \mathbf{i}}{\mathbf{a}_1 \cdot \mathbf{n}_2} N_3 \quad (\text{B2})$$

$$\text{where } \mathbf{a}_1 \cdot \mathbf{n}_3 = \frac{(x_3 - x_2)(y_2 - y_1) + (y_3 - y_2)(x_1 - x_2)}{[(x_3 - x_2)^2 + (y_3 - y_2)^2]^{1/2} [(x_2 - x_1)^2 + (y_2 - y_1)^2]^{1/2}}$$

$$\mathbf{a}_1 \cdot \mathbf{n}_2 = \frac{(x_3 - x_2)(y_3 - y_1) + (y_3 - y_2)(x_1 - x_3)}{[(x_3 - x_2)^2 + (y_3 - y_2)^2]^{1/2} [(x_3 - x_1)^2 + (y_3 - y_1)^2]^{1/2}} \quad (\text{B3})$$

$$N_2 = [(x_3 y_1 - x_1 y_3) + (y_3 - y_1)x + (x_1 - x_3)y] / d$$

$$N_3 = [(x_1 y_2 - x_2 y_1) + (y_1 - y_2)x + (x_2 - x_1)y] / d \quad (\text{B4})$$

After carrying out some algebraic simplification on the numerators of Eq.(B3), using Eqs.(A2), (B2)-(B4), the expression for the shape function F_{x1} can be written as

$$F_{x1} = \frac{(y_2 - y_1) N_2 [(x_3 - x_2)^2 + (y_3 - y_2)^2]^{1/2}}{x_3 y_2 - x_3 y_1 + x_2 y_1 + x_1 y_3 - x_2 y_3 - x_1 y_2 [(x_3 - x_2)^2 + (y_3 - y_2)^2]^{1/2}} + \frac{(y_3 - y_1) N_3 [(x_3 - x_2)^2 + (y_3 - y_2)^2]^{1/2}}{x_3 y_2 - x_3 y_1 + x_2 y_1 + x_1 y_3 - x_2 y_3 - x_1 y_2 [(x_3 - x_2)^2 + (y_3 - y_2)^2]^{1/2}}$$

$$F_{x1} = \frac{G}{x_3 y_2 - x_3 y_1 + x_2 y_1 + x_1 y_3 - x_2 y_3 - x_1 y_2} \quad (\text{B5})$$

where $G = (y_2 - y_1) N_2 + (y_3 - y_1) N_3$

$$= (y_2 - y_1) [(x_3 y_1 - x_1 y_3) + (y_3 - y_1)x + (x_1 - x_3)y] / d + (y_3 - y_1) [(x_1 y_2 - x_2 y_1) + (y_1 - y_2)x + (x_2 - x_1)y] / d$$

$$\text{or, } G = (y - y_1) [x_1 y_2 - x_2 y_1 + x_2 y_3 - x_3 y_2 - x_3 y_1 - x_1 y_3] / d \quad (\text{B6})$$

From Eqs.(B5) and (B6), we get

$$F_{x1} = (y_1 - y) [(x_3 - x_2)^2 + (y_3 - y_2)^2]^{1/2} / d$$

Similarly, F_{x2} and F_{x3} are given by

$$F_{x2} = (y - y_2) [(x_3 - x_1)^2 + (y_3 - y_1)^2]^{1/2} / d; \quad F_{x3} = (y_3 - y) [(x_2 - x_1)^2 + (y_2 - y_1)^2]^{1/2} / d$$

And the shape functions employed to approximate the y components of the fields are given by

$$F_{y1} = (x - x_1) [(x_3 - x_2)^2 + (y_3 - y_2)^2]^{1/2} / d; \quad F_{y2} = (x_2 - x) [(x_3 - x_1)^2 + (y_3 - y_1)^2]^{1/2} / d$$

$$\text{and } F_{y3} = (x - x_3) [(x_2 - x_1)^2 + (y_2 - y_1)^2]^{1/2} / d$$

Now, for comparison, the shape functions employed in Koshiba's element [12] for approximating the transverse field components are discussed here. For Koshiba's element, the edge shape functions are given by

$$\{F_x\} = [f_1 + g_1 y \quad f_2 + g_2 y \quad f_3 + g_3 y] \quad ; \quad \{F_y\} = [h_1 - g_1 x \quad h_2 - g_2 x \quad h_3 - g_3 x] \quad (\text{B7})$$

$$\text{where } f_k = [(y_{m+3} \cos \theta_{m+3} - x_{m+3} \sin \theta_{m+3}) \sin \theta_{l+3} - (y_{l+3} \cos \theta_{l+3} - x_{l+3} \sin \theta_{l+3}) \sin \theta_{m+3}] / \Delta$$

$$h_k = [(y_{l+3} \cos \theta_{l+3} - x_{l+3} \sin \theta_{l+3}) \cos \theta_{m+3} - (y_{m+3} \cos \theta_{m+3} - x_{m+3} \sin \theta_{m+3}) \cos \theta_{l+3}] / \Delta$$

$$g_k = [\cos \theta_{l+3} \sin \theta_{m+3} - \cos \theta_{m+3} \sin \theta_{l+3}] / \Delta$$

$$\Delta = \sum_{k=1}^3 (y_{k+3} \cos \theta_{k+3} - x_{k+3} \sin \theta_{k+3}) (\cos \theta_{l+3} \sin \theta_{m+3} - \cos \theta_{m+3} \sin \theta_{l+3})$$

$$0 \leq \theta_{k+3} = \tan^{-1} \frac{y_k - y_l}{x_k - x_l} < \pi$$

Here, (x_4, y_4) , (x_5, y_5) and (x_6, y_6) represent the mid point of the three sides of the triangle respectively and k, l, m progress cyclically around the three vertices of the triangle. Carrying out some trigonometric operations, the shape functions F_{x1} and F_{y1} for Koshiba's element are obtained as

$$F_{x1} = f_1 + g_1 y = \frac{(x_3 - x_1)(y_2 - y_3)(y_6 - y) - x_6(y_3 - y_1)(y_2 - y_3) - (x_2 - x_3)(y_3 - y_1)(y_5 - y) + x_5(y_2 - y_3)(y_3 - y_1)}{\Delta [(x_2 - x_3)^2 + (y_2 - y_3)^2]^{1/2} [(x_3 - x_1)^2 + (y_3 - y_1)^2]^{1/2}}$$

$$F_{y1} = h_1 - g_1 x = \frac{(x_2 - x_3)(y_3 - y_1)(x_6 - x) - y_6(x_3 - x_1)(x_2 - x_3) - (x_3 - x_1)(y_2 - y_3)(x_5 - x) + y_5(x_2 - x_3)(x_3 - x_1)}{\Delta [(x_2 - x_3)^2 + (y_2 - y_3)^2]^{1/2} [(x_3 - x_1)^2 + (y_3 - y_1)^2]^{1/2}}$$

The other shape functions also arrive at the similar expressions as above.